Arachnoid granulations — anatomy and imaging

Ian C Duncan
FFRad(D) SA

Unitas Interventional Unit
PO Box 14031
Lyttelton
0410

Arachnoid granulations were originally described by Pacchioni in 1705 and hence are also called Pacchionian granulations. They are specialised focal herniations of the arachnoid membrane, surrounding the brain, extending into the dural venous sinuses. They may also be found in association with the bridging veins that cross the subarachnoid space from the cerebral cortex to drain into the venous sinuses. Their function is thought to be the resorption of CSF into the circulation.[1,2] The arachnoid granulations extend into the sinus or adjacent venous lacunae through tight defects in the meningeal dura. The space in the centre of the granulation is in direct contact with the subarachnoid space. The endothelium of the sinus is reflected on the herniated granulation and may cover this structure entirely, or be deficient leaving a number of the arachnoid cells of the wall of the granulation in direct contact with the sinus lumen. These exposed cells are called arachnoid cap cells.[2,3] The granulations are responsible for the drainage of CSF from the subarachnoid space into the venous circulation. This forms a one-way valve between the relatively high pressure subarachnoid space and the lower pressure veins and sinuses. The actual transfer of fluid takes place partly through small intracellular channels in a passive manner, but mainly through active transport via a vacuole-mediated transcellular mechanism.[3,4] CSF is also absorbed to a much lesser degree through the leptomeninges in the spinal subarachnoid space. Arachnoid villi differ only from granulations in size, being much smaller. They are often only seen with the aid of magnification.[5,6] Arachnoid villi are present as early as the 26th week of pregnancy. They may be seen from the 39th week and are macroscopically evident (granulations) by 18 months of age.[7] Arachnoid granulations may therefore be derived from arachnoid villi.[2,8] They enlarge considerably by the age of 3 - 4 years[8] and continue to enlarge throughout adult life. They rarely grow larger than 1 cm in size and never larger than 2 cm. The larger ones can produce an erosion of the inner table of the adjacent calvarium. The depth of these 'depressions' may increase with increasing age.[5,9] Occasionally the 'depressions' may be deep enough to affect the outer table of the skull as well, and rarely 'giant' granulations may be seen.[10] Arachnoid granulations can calcify in later life.

Imaging of arachnoid granulations

The reported prevalence of arachnoid granulations in anatomic investigations varies considerably from 8.4% to 66%.[11,12] In these two series most were described as being present within the transverse sinuses. Grossman and Potts[5] found impressions in the skull due to arachnoid granulations in 46% of 400 randomly selected skull films. These increased in prevalence and depth with increasing age (Figs 1a, 1b). Most were seen in the anterior parietal region adjacent to the midline (average distance: 14 mm). They also reviewed 100 cerebral angiograms and found veins related to arachnoid granulations in 38%. In one further case there was a discrete filling defect in the superior sagittal sinus. No arachnoid granulations related to the transverse sinuses were noted. The reported incidence of arachnoid granulations with sectional imaging and angiography varies considerably from 0.3% to 90% (Table I). This considerable variability is related to various technical issues such as thicker scan slice thickness and lack of contrast administration during T1 weighted image acquisition in the earliest series.[13] The availability of higher imaging resolution together with contrast-enhanced imaging has led to greater imaging sensitivity and thus detection of arachnoid granulations (Fig. 1c).[14,15]

Descriptions of the anatomic locations of arachnoid granulations have also shown considerable variability, as shown in Table II. From these data, however, we can see that arachnoid granulations are found in relation to all major dural sinuses and many are related to bridging cortical veins or

Fig. 1a. Left external carotid digital subtraction angiogram. Slight misregistration of the mask allows visualisation of an indentation of the inner table of the skull at the site of an arachnoid granulation (arrow).

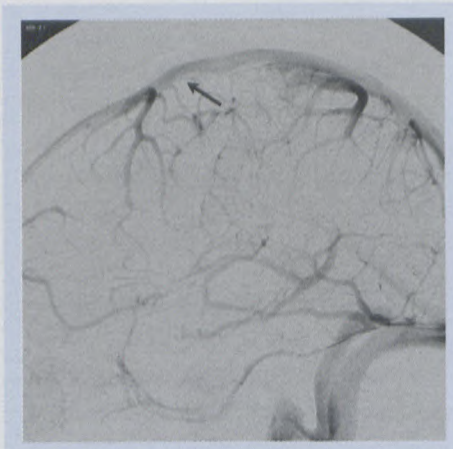

Fig. 1b. Selective left internal carotid arteriogram, late venous phase, showing slight indentation of the superior sagittal sinus at the site of the same granulation. (arrow)

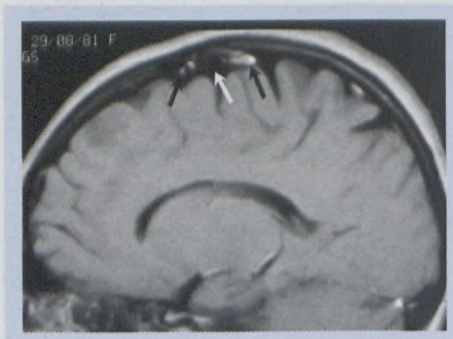

Fig. 1c. Parasagittal gadolinium-enhanced T1 MR scan showing the CSF-isointense granulation (white arrow) with associated enhancing cortical veins (black arrows).

cortical venous entry points (Figs 2a-e). One relatively common site of occurrence of an arachnoid granulation is at the confluence of the Vein of Labbe and the transverse sinus, seen in 21% of cases examined by Gailloud *et al.*[16] (Figs 3a, 3b). In the reports by Leach *et al.*[12] and Liang *et al.*,[15] granulations were also described in the straight sinus, typically at the junction of the sinus and the Vein of Galen (Figs 4a-g). The average number of arachnoid impressions seen on skull radiographs was shown by Grossman and Potts[5] to be 2.7 in patients over 19 years of age, with the number and depth of the impressions also increasing with increasing age. Calcification of granulations was reported by Roche and Warner[13] in 3 of 31 cases seen at CT and 1 of 18 cases seen at MRI (8%). No calcified granulations were seen in the cases reviewed by Leach *et al.*[12] An interesting discrepancy between angiographic studies and sectional imaging is that the former commonly describe the presence of arachnoid granulations in or close to the superior sagittal sinus which tend not to present typically as intraluminal filling defects within the sinus, whereas those in the transverse and other sinuses do protrude into the sinuses seen as discrete intrasinus filling defects on sectional imaging. The CT density of granulations varies from being isointense with CSF to being isointense with brain. They do not enhance after contrast administration, being seen as discrete hypointense filling defects surrounded by enhanced blood within the sinus.[12-14] With MR imaging, granulations are typically hypointense relative to brain and isointense to CSF on T1-weighted and on fluid-attenuated inversion recovery (FLAIR) sequences (Figs 1c, 4a-c). They are again non-enhancing, being seen as discrete hypointense filling defects within the sinuses on contrast enhanced T1-weighted images.[12-15] Calcified granulations may appear isointense with parenchyma on T1-weighted images and hypointese relative to CSF on T2-weighted images.[13] The size of granulations can vary between 1 and 14 mm (average 2 - 7 mm), with the largest being found in relation to the transverse sinuses.[10,12,13,15] 'Ectopic' granulations have been described presenting in the convexity of the skull some distance from the sagittal sinus,[17] although Grossman and Potts[5] showed the presence of arachnoid impressions in randomly selected individuals up to 28 mm from the midline.

The most important differential diagnosis for these granulations by virtue of the appearances as intra-

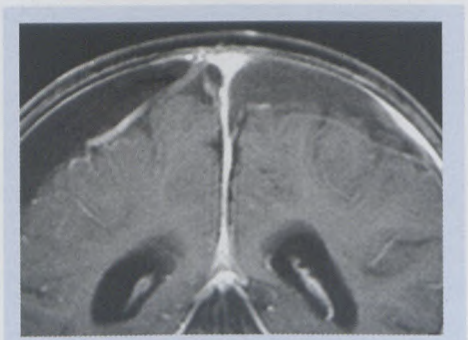

Fig. 2a. Coronal gadolinium-enhanced T1 MR scan showing the passage of the 'bridging' segment of the cortical veins traversing the arachnoid spaces exaggerated by the presence of bilateral chronic subdural fluid collections (arrow).

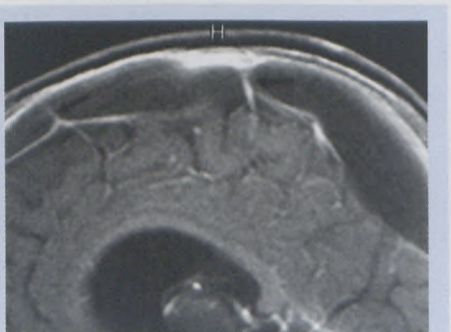

Fig. 2b. Sagittal image, same case, again showing the bridging veins traversing the arachnoid spaces (arrows). No arachnoid granulations are macroscopically evident in this patient who is 2 years old.

Table I. Studies showing the prevalence of arachnoid granulations with imaging

Study	Imaging methods	Results	Estimated prevalence (%)
Roche & Warner[13]	CT, MR, MRA, DSA	9/3100 on CT 2/200 on MR	0.3 - 1%
Leach et al.[12]	Contrast-enhanced CT, MR, cadaveric specimens	138/573 on CECT (24%) 13/100 on CEMRI (13%) 19/29 cadavers (66%)	24 - 66
Casey et al.[14]	CT venography	11/20 on CT venography	55
Gailloud et al.[16]	Cerebral angiography	12/57 patients	21.1
Liang et al.[15]	MRI (contrast-enhanced 3D MPRAGE)	90/100 patients	90

Fig. 2c. Selective left internal carotid digital subtraction arteriogram, left anterior oblique projection, showing a well-circumscribed filling defect indenting the bridging segment of a cortical vein (arrow). This appearance is typical of an arachnoid granulation.

Fig. 2d. Same arteriogram, PA projection. The granulation is visible parasagittally (arrow) .

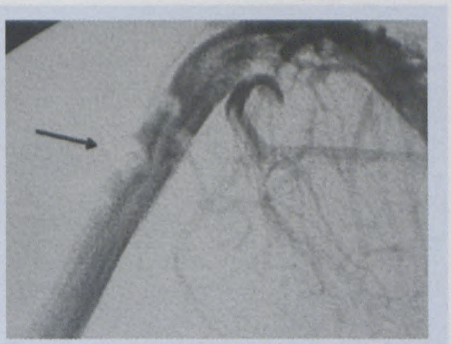

Fig. 2e. Selective left internal carotid arteriogram, late venous phase, in another patient showing multiple filling defects protruding into the superior sagittal sinus lumen itself (arrow). These are also compatible with granulations.

Table II. Anatomic location of arachnoid granulations

Study	Method	Anatomical location	Cortical vein association
Grossman & Potts[5]	Cerebral angiography	All parasagittal (Av:14 mm) Mainly anterior parietal	38/100 (38%)
Roche & Warner[13]	CECT, MRI, MRA, DSA	Transverse sinus: 85% Torcula: 5% Sigmoid sinus : 10%	16/41 (39%)
Leach et al.[12]	CECT, MRI	Right transverse sinus: 39% Left transverse sinus: 52% Sigmoid sinus: 2% Torcula: 5% Distal superior sagittal sinus: 0.6% Straight sinus: 1%	95/154 on CT (62%) 11/13 on MRI (85%)
Casey et al.[14]	CT venography	Mostly transverse sinus	Not mentioned
Gailloud et al.[16]	Cerebral angiography	Transverse sinus at the confluence of the vein of Labbé	12/12 (100%)
Liang et al.[15]	3D Contrast-enhanced MPRAGE MRI	Superior sagittal sinus: 53.8% Transverse sinus: 28.1% (Right transverse sinus: 11%) (Left transverse sinus: 17.1%) Straight sinus: 17.6% Vein of Galen: 0.5%	414/433 (96%)

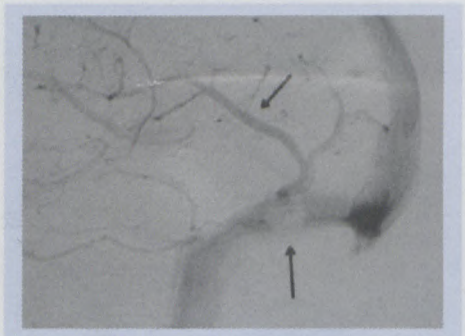

Fig. 3a. Selective left internal carotid arteriogram, late venous phase, showing a filling defect compatible with a granulation related to the confluence of the vein of Labbé and the lateral transverse sinus (arrows).

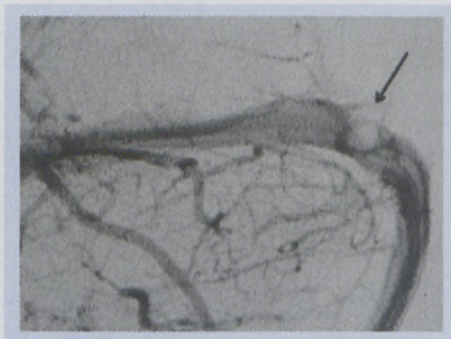

Fig. 3b. Same arteriogram, Towne's projection, showing the granulation in the distal or lateral aspect of the left transverse sinus (arrow).

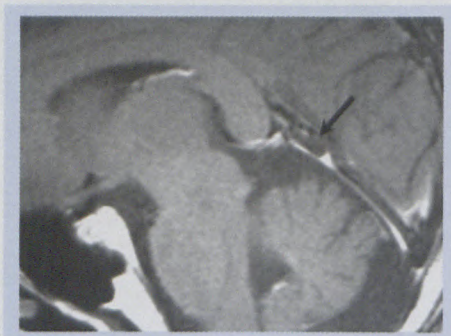

Fig. 4a. Median sagittal gadolinium-enhanced T1 weighted MR scan showing a discrete unenhancing filling defect within the proximal straight sinus (arrow).

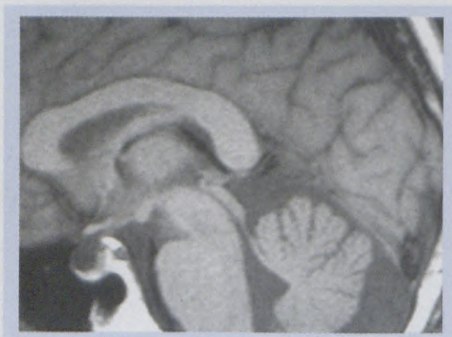

Fig. 4b. The same 'lesion' is invisible on the corresponding unenhanced scan, being isointense with CSF.

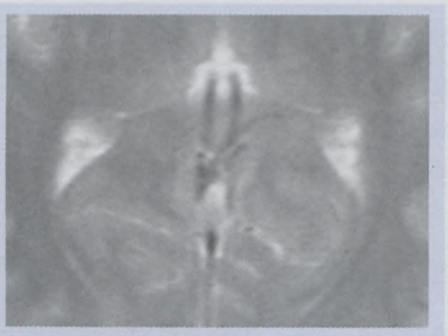

Fig. 4c. No signal abnormality is seen on the axial T2 image of this region.

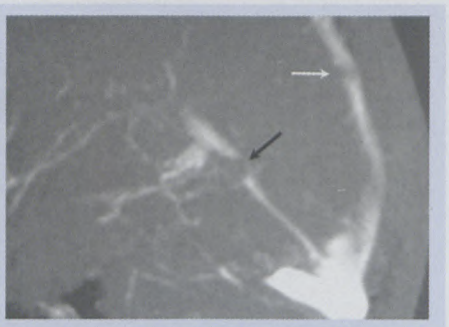

Fig. 4d. MR venogram showing the same intrasinus filling defect (black arrow). Note a second filling defect in the posterior aspect of the superior sagittal sinus (white arrow).

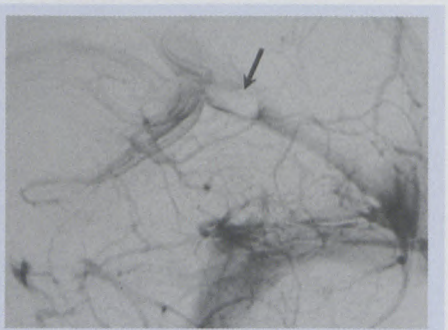

Fig. 4e. Late venous return phase, lateral projection, of a selective vertebral arteriogram showing the same filling defect in the proximal straight sinus (arrow) compatible with an arachnoid granulation.

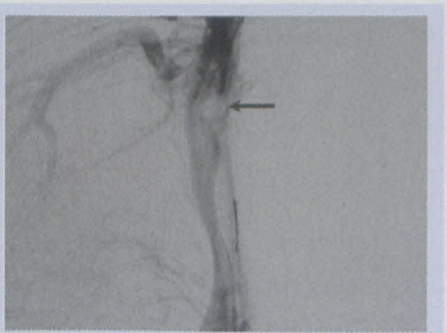

Fig. 4f. Late venous return phase of a right internal carotid arteriogram, PA projection, shows the filling defect in the distal superior sagittal sinus (arrow).

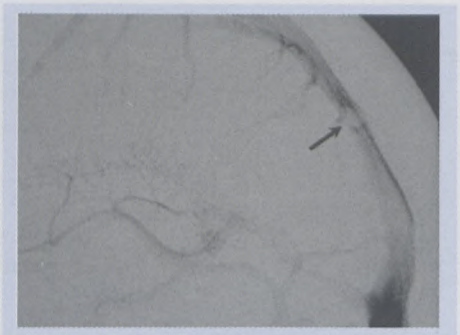

Fig. 4g. Same arteriogram, lateral projection, showing the same (probable) granulation (arrow).

sinus filling defects is sinus thrombosis. In general the granulations preferentially appear as rounded or ovoid well-circumscribed discrete filling defects, whereas thrombi tend to be more irregular and possibly adherent to the sinus wall, with proximal or distal extension due to thrombus propagation (Figs 5a-h). Furthermore, the signal intensity of thrombus differs from that of CSF on both T1-and T2 weighted images.[18] Because of the strong relationship between granulations and bridging veins, such an association may not be seen in the case of sinus thrombosis. Intra-sinus septa can occasionally be identified but are linear structures and easily differentiated from the rounded granulations.[15] Other rare lesions that may produce polypoidal filling defects within a sinus include nodules of ectopic tissue (hamartomas).[19]

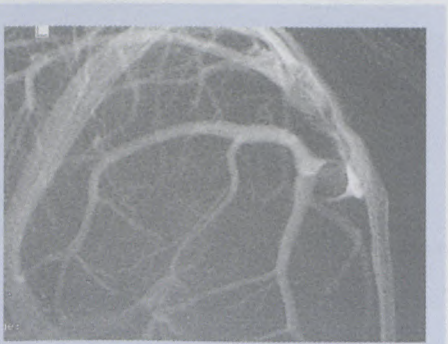

Fig. 5a. Selective right internal carotid arteriogram, right anterior oblique projection, showing a rounded filling defect in the bridging part of a cortical vein compatible with arachnoid granulation.

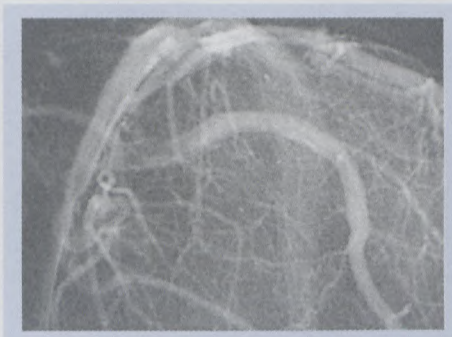

Fig. 5b. Selective left internal carotid arteriogram, left anterior oblique projection, in another patient, showing an ill-defined filling defect perhaps more likely to indicate a cortical vein thrombosis (treated as such but never confirmed by other means).

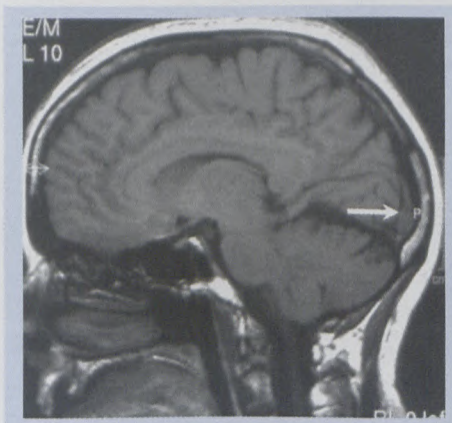

Fig. 5c. Unenhanced T1 median sagittal scan showing a focal hyperintense signal in the distal superior sagittal sinus of another patient, suspected of being a thrombus (arrow).

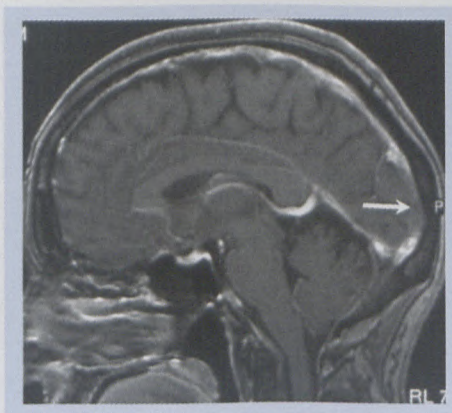

Fig. 5d. Same case, median sagittal gadolinium-enhanced T1 image, showing an elongated filling defect in the same position.

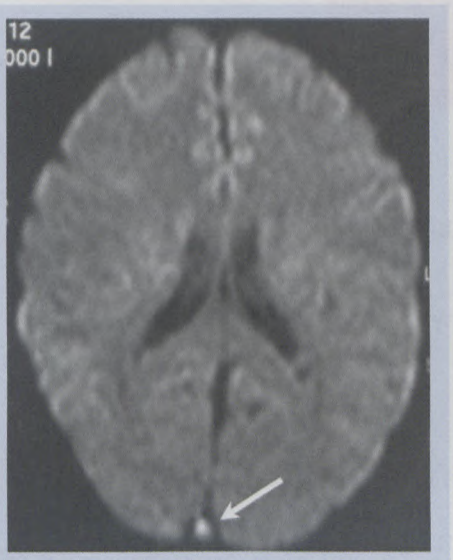

Fig. 5e. Axial FLAIR image showing hyperintense signal within the sinus in keeping with thrombus (arrow).

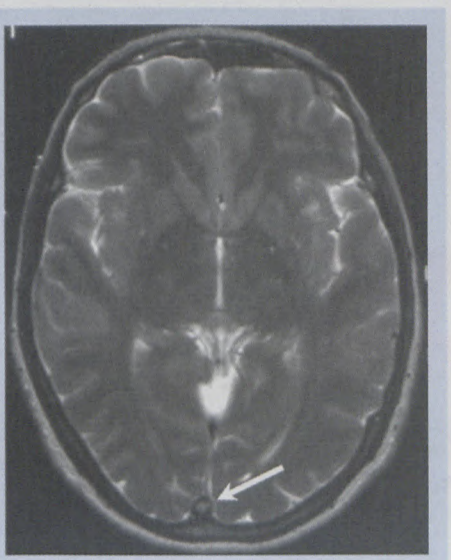

Fig 5f. Axial T2 weighted image again showing a focal signal hyperintensity in the distal sagittal sinus (arrow).

Fig. 5g. Posterior coronal gadolinium-enhanced T1 image showing the linear extent of the thrombus above the torcula (arrow).

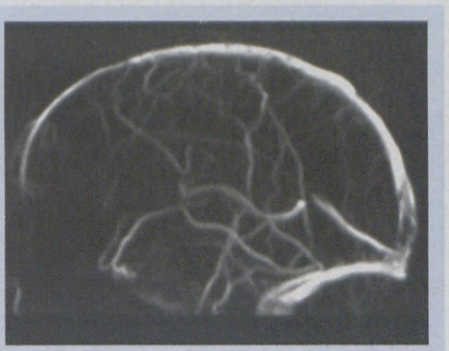

Fig. 5h. Confirmation of the thrombus within the sinus is also provided by MR venography. All symptoms resolved after treatment with heparin.

Conclusion

In conclusion, arachnoid granulations are now readily identifiable with modern sectional imaging and digital subtraction angiography and their presence can result in the erroneous diagnosis of intracranial masses or cysts or intra-sinus thrombosis in some settings. Knowledge of their imaging appearance, anatomical site and association with cortical veins and venous confluences with the dural sinuses will all assist with their correct identification and exclusion as possible abnormal or pathological entities.

References

1. Jayatilaka AD. Arachnoid granulations in sheep. *J Anat* 1965; **99:** 315-327.
2. Upton ML, Weller RO. The morphology of cerebrospinal fluid damage pathways in human arachnoid granulations. *J Neurosurg* 1985; **63:** 867-875.
3. Corbett JJ, Haines DE, Aral MD. The ventricles, choroid plexus and cerebrospinal fluid. In: Haines DE, ed. *Fundamental Neuroscience.* Philadelphia: Churchill Livingstone, 2002: 94-106.
4. Benarroch EE, Westmoreland BF, Daube JR, Reagan TJ, Sandok BA, eds. *Medical Neurosciences: An Approach to Anatomy, Pathology and Physiology by Systems and Levels.* Philadelphia: Lippincott Williams and Wilkins, 1999: 125-150.
5. Grossman CB, Potts DG. Arachnoid granulations: radiology and anatomy. *Radiology* 1974; **113:** 95-100.
6. Potts DG, Reilly KF, Deonarine V. Morphology of the arachnoid villi and granulations. *Radiology* 1972; **105:** 333-341.
7. Gómez DG, Dilbenedetto AT, Pavese AM, Firpo

A, Hershan DB, Potts DG. Development of arachnoid villi and granulations in man. *Acta Anat* 1981; **111:** 247-258.

8. Le Gros Clark WE. On the Pacchionian bodies. *J Anat* 1920; **55:** 40-48.
9. Basmanjian JV. The depressions for the arachnoid granulations as a criterion of age. *Anat Rec* 1952; **112:** 843-845.
10. Mamourian AC, Towfighi J. MR of giant arachnoid granulation, a normal variant presenting as a mass within the dural venous sinus. *Am J Neuroradiol* 1995; **16:** 901- 904.
11. Browder J, Kaplan JH, Howard J. Hyperplasia of pacchionian granulations. *Arch Pathol* 1973; **95:** 315-317.
12. Leach JL, Jones BV, Tomsick TA, Stewart CA, Balko MG. Normal appearance of arachnoid granulations on contrast-enhanced CT and MR of the brain: Differentiation from dural sinus disease. *Am J Neuroradiol* 1996; **17:** 1523-1532.
13. Roche J, Warner D. Arachnoid granulations in the transverse and sigmoid sinuses: CT, MR and MR angiographic appearance of a normal anatomic variation. *Am J Neuroradiol* 1996; **17:** 677-683.
14. Casey SO, Ozvath R, Choi JS. Prevalence of arachnoid granulations as detected with CT venography of the dural sinuses. *Am J Neuroradiol* 1997; **18:** 993-994.
15. Liang L, Korogi Y, Sugahara T, *et al.* Normal structures in the intracranial dural sinuses: Delineation with 3D contrast-enhanced magnetization prepared rapid acquisition gradient-echo imaging sequence. *Am J Neuroradiol* 2002; **23:** 1739-1746.
16. Gailloud P, Muster M, Khaw N, *et al.* Anatomic relationship between arachnoid granulations in the transverse sinus and the termination of the vein of Labbé: an angiographic study. *Neuroradiology* 2001; **43:** 139-143.
17. Kuroiwa T, Takeuchi E, Tsutsumi A. Ectopic arachnoid granulomatosis: A case report. *Surg Neurol* 2001; **55:** 180-186.
18. Zimmerman RD, Ernst RJ. Neuroimaging of cerebral venous thrombosis. *Neuroimaging Clin N Am* 1992; **2:** 463-485.
19. Kollar C, Johnston I, Parker G, Harper C. Dural arteriovenous fistula in association with heterotopic brain nodule in the transverse sinus. *Am J Neuroradiol* 1998; **19:** 1126-1128.